UPPER CARBONIFEROUS MUDROCKS, MALTON, YORKSHIRE, ENGLAND AND THEIR UNCONVENTIONAL HYDROCARBON POTENTIAL

M. Slowakiewicz[*1,2], C. H. Vane[3], M. E. Tucker[4] and R.D. Pancost[1]

[1] Organic Geochemistry Unit, The Cabot Institute, School of Chemistry, University of Bristol, Cantock's Close, Bristol, BS8 1TS.

* corresponding author, m.slowakiewicz@gmail.com.

[2] Polish Geological Institute, ul. Rakowiecka 4, 00-975 Warsaw, Poland.

[3] British Geological Survey, Keyworth, Nottingham, NG12 5GG.

[4] Department of Earth Sciences, University of Bristol, Bristol, BS8 1RJ.

In order to investigate the shale-gas potential of Upper Carboniferous (Namurian) black shales in the upper Bowland-Hodder unit in the Cleveland Basin, Yorkshire (northern England), a cored section from the Malton-4 well was selected for multidisciplinary analysis complemented by geochemical (Rock-Eval pyrolysis and biomarkers) and sedimentological data. The black shales are interbedded with bioturbated and bedded sandstones ("Millstone Grit") and represent offshore-basinal to prodelta lithofacies. The total organic carbon (TOC) content of the black shales ranges from 0.37 to 2.45 wt %. Rock-Eval pyrolysis data indicate that the organic matter is mainly composed of Type II and III kerogen. Tmax (436-454oC), and 20S/(20S+20R) and ββ/(ββ+αα) C29 sterane ratios indicate that organic matter is in the early- to mid-mature stage with respect to hydrocarbon generation. Sedimentological and geochemical redox proxies indicate that the black shales were deposited in periodic oxic-dysoxic and probably anoxic bottom waters with at least episodic oxic conditions, explaining the relatively low TOC values. Deposition of the shales took place in a moderately deep basinal - prodelta setting, and bioturbated sandstones represent prograding delta-front facies. The Rock-Eval parameters suggest that the mudrocks have a limited shale-gas potential and that a shale-oil resource can be ruled out.

Key words: black shale, shale gas, biomarker characterization, organic matter, thermal maturity, hydrocarbon potential, Cleveland basin, Carboniferous, Yorkshire, England.

INTRODUCTION

Organic-rich black shales are important source rocks and may also serve as seals for conventional oil and gas reservoirs. Recent advances in drilling and completion technology, specifically horizontal drilling and hydraulic fracturing ("fracking"), have made the production of natural gas from shales economic. Shale gas is an unconventional gas-system in which the shale is both the source of, and reservoir for, natural gas [Jarvie, 2012]. The gas is derived from the organic matter within the shale as a result of biogenic and/or thermogenic processes.

In the USA, annual shale-gas production reached 7.85 tcf in 2011, approximately 34% of dry gas production (www.eia.gov). Major gas-producing shales in the USA are organic-rich (total organic carbon, TOC = 0.45 – 25 %), early mature to highly overmature (vitrinite reflectance, R_r = 0.4 – 3.4 %) and buried to variable depths (150 - 3350 m) (Jarvie, 2012). As shale is the most abundant sedimentary rock on Earth, shale gas resources have also been investigated in other countries [e.g. Boyer et al., 2011; Jarvie, 2012]. In addition, liquid oil ("tight oil") may also in theory be extracted from organic-rich shales, whose poroperm properties prevent the oil from escaping.

Gas shales and tight-oil shales have a higher potential for commercial hydrocarbon production if the shales contain significant proportions of brittle framework grains such as quartz and feldspar (~>30%) and also carbonate, rather than being dominated by clay minerals (Bunting and Breyer, 2012; Jarvie, 2012). The presence of brittle grains allows the shales to be fractured more easily during reservoir development operations.

In the UK, organic-rich shales of Cambrian to Jurassic ages, deposited in marine, transitional marine and lacustrine settings, are widely distributed. Smith et al. (2011) described Lower Palaeozoic shale basins on the English Midland microcraton, Lower

Carboniferous (Mississippian) shales in the Central Pennine Basin, and Upper Carboniferous (Pennsylvanian) shales in the Stainmore and Northumberland basins. These authors concluded that the Mississippian Hodder Mudstone Formation and Bowland Shale Formation (informally referred to as the Bowland –Hodder unit) may constitute the most prospective shale-gas play. Andrews (2013) calculated that the Bowland-Hodder shale-gas play in north-central Britain may include gas resources totalling 822 to 2281 tcf, although these estimates refer to the volume of gas contained in the shale strata, not the volume of gas which can be recovered. These estimates of gas in-place can be viewed as preliminary in view of the lack of reliable data on gas content and recoverable gas reserves. In addition, incomplete or scarce information on kerogen type, original hydrogen index (HI) values, mineralogy, gas content, porosity and pressure values for the Bowland-Hodder shales make the calculation of recoverable gas reserves uncertain.

In the present paper, we focus on geological and geochemical analyses of a cored section of the Carboniferous (Namurian) Bowland-Hodder unit from the Malton-4 well in the Cleveland Basin, northern England (Fig. 1). Based on the results, the shale-gas potential of the cored section is described and evaluated.

GEOLOGICAL AND TECTONIC FRAMEWORK

During the Carboniferous the UK was situated at low latitudes to the north of the Rheic Ocean. Carbonates and coarse clastics were deposited in extensive shallow seas and deeper-water areas were dominated by mudrocks (George et al. 1976; Waters et al. 2007). The Early Carboniferous (Mississippian) was a time of north-south extension which resulted in a series of positive blocks/platforms (mostly underlain by Caledonian granite) and rapidly subsiding basins. This was followed in the Late Carboniferous (Pennsylvanian) by more regional subsidence and then a phase of compression, culminating with latest Carboniferous -- Early Permian deformation and inversion (Gawthorpe et al., 1989; Fraser and Gawthorpe, 1990).

In northern England, Fraser and Gawthorpe (1990, 2003) identified a syn-rift megasequence (Upper Devonian to upper Brigantian: EC in Fig. 2), followed by a post-rift megasequence (LC) from the upper Brigantian to the upper Westphalian C. Within these two megasequences, sequences were distinguished based on minor changes in tectonic regime: EC1 through EC6 and LC1 (a/b/c) and LC2 (Figs 2, 3).

Platform areas in northern England are from north to south the Cheviot, Alston, Askrigg and Market Weighton blocks; these are separated by the Northumberland, Stainmore-Cleveland and Bowland-Craven-Pennine-Leeds basins (Gawthorpe et al., 1989; Dean et al., 2011).. In the latest Early Carboniferous (Asbian-Brigantian) to early Namurian (sequences EC4 through LC1a/b), deltas gradually advanced and prograded southwards from the Scottish Borders -- Southern Uplands region, depositing mudrock-sandstone units across shallow-water carbonates (Johnson, 1984; Dean et al., 2011). As a result of orbitally-forced sea-level fluctuations, numerous (~70) Yoredale "cycles" were generated comprising shallow-marine limestone passing up into prodelta mudrock then delta-front and delta-plain sandstones, locally with coals (Tucker et al., 2009). Thinner successions were deposited on the platforms, and thicker, mudrock-dominated successions in the basins.

In the Cleveland-Leeds basins in NE Yorkshire, shales of the Bowland-Hodder unit were deposited in the Brigantian to early Namurian (EC6-LC1a/b) until the deposition of coarser-grained clastics ("Millstone Grit") derived from the prograding delta-plain system from the north-NE (Fig. 4) (Johnson, 1984; Dean et al., 2011). The shales in the Cleveland Basin are organic-rich, as shown by the presence of oil-shows and high gamma responses (150-180 API) recorded in the Seal Sands borehole near Hartlepool [locate it in Fig. 1] (Johnson et al., 2011).

The Malton-4 well was drilled during exploration for gas in the Permian Zechstein in 1985, and the Permian-Carboniferous boundary occurs at a depth of 5149 ft (1569.4 m; Fig. 5. Some 17.5 metres of Carboniferous strata were cored and recovered, and the facies are described below. In terms of stratigraphy, the core is probably located in the

upper part of the Bowland-Hodder unit (Arnsbergian) within the LC1b sequence of Fraser and Gawthorpe (1990).

SAMPLES AND METHODS

Five shale core samples from the Upper Carboniferous succession of the Malton-4 well were collected for sedimentological, petrographic and organic geochemical analyses. For SEM, freshly broken surfaces were coated with silver to observe micro- and nano-sized pores in the black shales and also their petrographic composition. A high vacuum and partial vacuum (10Pa - 10-4Pa) JEOL JSM 5600 LV scanning electron microscope (SEM) was used with a secondary electron detector based on the scintillator-photomultiplier design of Everhardt & Thornley. The SEM was also fitted with a solid-state backscattered electron detector used for compositional and topographical information and energy-dispersive spectrometry (EDS) for elemental analysis. Accelerating voltages between 1 - 30KV were used.

Rock Eval pyrolysis/TOC analysis

Samples were analysed using a Rock-Eval 6 analyser configured in standard mode (pyrolysis and oxidation as a serial process). Powdered drill-core samples (60 mg /dry wt) were heated from 300ºC to 650ºC at 25ºC/min in an inert atmosphere of N2 and the residual carbon then oxidised at 300ºC to 850ºC at 20ºC/min (hold 5 min). Hydrocarbons released during the two-stage pyrolysis were measured using a flame ionization detector and CO and CO2 measured using an IR cell. The performance of the instrument was checked every 10 samples against the accepted values of the Institut Français du Pétrole (IFP) standard (IFP 160 000, S/N1 5-081840). Rock-Eval parameters were calculated by integration of the amounts of HC (thermally-vaporized free hydrocarbons) expressed in mg/HC/g rock (S1) and hydrocarbons released from cracking of bound OM expressed in mg/HC/g rock (S2) (Engelhart et al., 2013). The Hydrogen Index (HI) was calculated from S2 x 100/TOC and the Oxygen Index (OI), S3 x 100/TOC. However comparative analyses of shales and extracted kerogens by Rock-Eval 6 versus an acid washed /

elemental analyzer (Leco SC-444) suggested that although there was a strong overall correlation (r2 = 0.95), the former method slightly underestimates whole rock TOC (Behar et al., 2001).

Biomarker Characterisation

Gas chromatography (GC) and gas chromatography – mass spectrometry (GC-MS) analyses were conducted on extracts obtained from the five samples. Powdered (20 g) core samples were extracted using a Soxhlet apparatus with 200 ml dichloromethane:methanol (9:1, v/v) for 24 h; copper was added to the round-bottomed flask to remove elemental sulphur. Aliquots of total lipid extract were separated into polar and apolar fractions using a column with activated silica gel (230-400 mesh, 4 cm, bottom). Elution proceeded with 3 ml hexane (saturated fraction), hexane:dichloromethane (3:1, v/v; aromatic fraction), and 5 ml methanol (polar fraction), respectively.

1 µl aliquots of each fraction were analysed by GC using a Hewlett Packard Series II 5890 instrument, fitted with an on-column injector and a capillary column with a CP Sil5-CB stationary phase (60 m x 0.32 mm, df = 0.10 µm). Detection was achieved with flame ionisation (FID) with helium as the carrier gas. The temperature programme consisted of three stages: 70-130 °C at 20 °C per min rate; 130-300 °C at 4 °C per min; and 300 °C at which the temperature was held for 10 min. GC-MS analyses were performed using a ThermoQuest Finnigan Trace GC-MS fitted with an on-column injector and using the same column and temperature programme as for GC analyses. The detection was based on electron ionization (source at 70 eV and scanning range 50-580 Daltons), and compounds were identified by comparison of retention times and mass spectra to the literature.

RESULTS AND DISCUSSION

Sedimentology

185 The 17.5 m core consists of shales and sandstones; apart from a 0.6 m section, the core is
186 virtually complete (Fig. 5). Four major lithofacies can be distinguished: (i) mudrock, (ii)
187 sandy mudrock, (iii) bioturbated sandstone and (iv) "massive" sandstone. These
188 lithofacies are arranged into several packages.
189
190 The *mudrock* lithofacies ranges from mudstone to siltstone, and from laminated and
191 fissile shale to blocky and massive mudstone. "Poker-chip" shale with a weak lamination
192 (the name refers to its fissility) also occurs. The colour is in general black although some
193 layers are dark grey. Lamination is at a mm-scale (Fig. 6a) and is defined by sub-mm
194 partings of clay, organic matter and muscovite. The laminae are composed of silt-sized
195 quartz grains, well-sorted with an average grain-size of 20 μm. Organic matter is present
196 as lamina-parallel and impersistent streaks and along stylolite seams. Pyrite crystals and
197 framboids are common. Burrows are mostly absent, although local ovoid and elongate
198 patches of clay-rich, silt-poor sediment are probably small burrow fills (Fig. 7). More
199 massive mudrocks are non-laminated. From thin-section the typical composition of the
200 shales is 60% clay matrix, altered feldspar and other grains, 30% quartz silt grains, 5%
201 mica (mostly muscovite) and 5% opaque grains and dark streaks (pyrite crystals and
202 framboids, and organic matter which can be distinguished in reflected light) (Fig. 8).
203 Pellets of clay, 10 microns in diameter and commonly flattened, were observed. In the
204 core, the mudrocks form units up to 5 m thick.
205
206 SEM examination together with EDS of the shale indicates the presence of quartz, clay
207 minerals, pyrite and organic matter (Fig. 9). Although some plucking of grains is likely to
208 have occurred, pores are clearly observed within and between clay flakes, within the
209 organic matter, and between silt grains (Figs 8a-c, 9). Micron-sized pyrite framboids are
210 common and some porosity is present between crystallites (Fig. 8d, 9a). XRD analysis of
211 the mudrocks indicated that quartz is dominant in some samples, and that chlorite and
212 illite are present in variable quantities. Muscovite is also present.
213
214 *Sandy mudrock* was present as a minor component and consists of planar- and cross-
215 laminated thin beds of quartz silt to fine sand within the dark mudrock. One 5 cm thick

unit of fine sand may be a storm bed or tempestite (Fig. 6b). Cm-size sand-filled *Planolites*-type burrows are common within dark grey-black mudrock. The sandy mudrock units are mostly less than 20 cm in thickness and are in general transitional between black mudrock and lighter-coloured sandstone.

Bioturbated sandstone is fine to medium-grained, sometimes with a low mud content (up to ~20%) present as streaks and wisps associated with burrow structures (Fig. 6c,d). The sandstones are characterised by well-developed trace fossils as well as more vague bioturbation structures. *Ophiomorpha* tubes 1-2 cm in diameter and filled with sand are present and are lined by clay, 1-2 mm thick. *Thalassinoides* are larger nodular structures, 2-3 cm in diameter, with vague internal laminae (Fig. 6c). Both *Ophiomorpha* and *Thalassinoides* are probably the result of burrowing by crustaceans. Some bioturbated areas have curved, convex-up closely stacked clay laminae, up to 3 cm across, and are interpreted as burrows due to the activity of bivalves such as *Pelecypodichnus* and *Lockeia* (Fig. 6d). Simple *Planolites* burrows have a weak internal structure, cm-thick curved and cross-cutting, and are oriented horizontally across the core (Fig. 6d).

"Massive sandstones" are cream to white in colour and in the cut, but unpolished core appears structureless or has only faint lamination/bedding. Cross- and planar- bedding and bioturbation may be present but these features are difficult to resolve. Some sharp surfaces are present indicating erosion and scour. Units of this facies are up to 1 m thick.

Facies stacking and interpretation

Two coarsening-upward units can be recognised in the core studied (Fig. 5). In the lower part of the core (1586-1579 m depth), ~5 m of mudrock with "poker chip" facies passes up through sandy mudrock into bioturbated and "massive" sandstone. An overlying unit (1579-1576 m depth) also shows a coarsening-up package into massive sandstone. The upper part of the core mostly consists of bioturbated sandstone and interbedded mudrock.

The two coarsening-upward packages probably represent prograding delta-front facies, from basinal-prodelta muds through to mouth-bar sands. The black, organic-rich nature of the mudrocks could indicate suboxia-anoxia in a stratified basin as has been suggested for contemporaneous basin facies elsewhere in UK (e.g. Fraser and Gawthorpe, 1990; Andrews, 2013). The sandy mudrocks are shallower-water deposits and the presence of discrete muddy sand beds with planar- and cross- lamination could indicate a storm influence (tempestites) or distal hyperpycnal flows from rivers (Fig. 6b). The bioturbated sand facies indicates intermittent sand supply, allowing sediment reworking by an infauna in a distal to medial mouth-bar setting. The more massive sands are interpreted to have been deposited in a more-proximal higher-energy mouth bar setting, where subaqueous distributary/river-outflow currents and waves reworked the sand. At this time (in the early Namurian), the delta front with distributary channels and bays, shoreline sands and delta-top channels and coal-forming swamps-mires were located some way to the north and NE in the Cleveland Basin, but the delta system was prograding to the south.

The Upper Carboniferous mudrock facies observed in the studied core is similar to those described from age-equivalent shale-gas formations, including the Barnett Shale (Mississippian, Texas: Abouelresh and Slatt, 2012) and other mud-rich successions (e.g. Plint, 2014, for a Cretaceous pro-delta system).

Total organic matter

The total organic matter content (TOC % wt/wt) within the Upper Carboniferous mudrocks of Malton-4 ranged from 0.37 to 2.45 % with an arithmetic mean of 1.57 % (Table 1). This mean is influenced by one outlier at 0.37 % obtained from the uppermost part of the succession close to the boundary with the Rotliegend sandstones. In general, TOC values at or greater than 2 % appear to indicate a potentially viable shale-gas resource (Andrews, 2013 and references therein). In addition, the presence of clay minerals may reduce S1 and S2 values in samples with TOC values less than 2.0 %. Therefore, this suggests that the mudrocks from 1570.3-1579.5 m may have potential as

277 an unconventional shale-gas resource, whereas samples at 1569.4 and 1583.1 m fall
278 below the TOC threshold. Overall, the potential for shale gas is based upon just one
279 sample and that higher resolution sampling for Rock-Eval analysis is required before a
280 definitive conclusion can be drawn.
281
282 The low TOC values in the upper part of the latter thickness range may be due to the
283 post-depositional, early-diagenetic aerobic oxidation of sedimentary organic matter,
284 known as burn-down (Kodrans-Nsiah et al., 2009). Burn-downs have been postulated to
285 explain decreasing TOC and palynomorph concentrations in turbidite sediments off Cape
286 Verde and Mediterranean sapropels (Thomson et al., 1995; Robinson, 2001), the process
287 suggests a strong preservation control on organic matter accumulation as compared to
288 changes in productivity and is initiated by an influx of oxygenated bottom water and
289 sediment pore water which then drives aerobic oxidation of the organic matter that was
290 already deposited. In this current work, a similar burn-down event maybe plausible
291 particularly if the overlying Rotliegend sandstones were deposited in oxidising conditions
292 but not were rapidly buried.
293
294 The TOC values presented here for the Upper Carboniferous mudrocks from the Malton-
295 4 well fall within the range previously reported for the Bowland-Hodder unit (TOC = 1-3
296 %), but do not equal the high TOC values of up to 8 % reported in some Namurian shales
297 in the UK (Andrews, 2013).
298
299 **Maturity of the organic matter**
300 In sedimentary rocks thermal maturity can be measured by vitrinite reflectance (Rr) and
301 an equivalent can be estimated using Rock-Eval (Tmax) values. In this study (Table 1),
302 Tmax values ranged from 436 to 454oC which is approximately equivalent to Rr of 0.70
303 – 1.01 (Jarvie et al., 2001). Taking the arithmetic mean of % Rr (estimated) of 0.85 (±
304 0.13), the black shales analysed fall in the middle of the oil window (Rr 0.6-1.0). Wet-gas
305 generation, that is gas containing >12 % of non-methane gas, is generally taken to begin
306 at 450 °C or about 1.0% Rr. Thus the black shales appear to be of sufficient maturity to
307 have generated liquid oil and possibly some wet gas but are not sufficiently mature

enough to have generated significant amounts of dry gas (above about 470 oC ≈ Rr 1.4 %).

Values of the production index PI = S1/(S1 + S2) for the shale samples ranged from 0.05 to 0.15 (Table 1). The PI typically increases with depth and also increases prior to expulsion; it is therefore correlated with maturity. Here, the PI indicates at least early oil window maturity (Peters and Cassa, 1994).

The 20S/(20S+20R) and ββ/(ββ +αα) sterane ratios increase with maturity and reach equilibrium values of 0.55 and 0.70, respectively, and can be used for maturity evaluations (Mackenzie et al., 1980). 20S/(20S+20R) and ββ/(ββ +αα) sterane ratios for shale samples are 0.42-0.56 and 0.40-0.55 respectively, which indicate that organic matter is at the early- to mid-mature stage (Table 2). 20S/(20S+20R) sterane ratios (0.53-0.56) in two samples show that epimerisation at the C20 position has been completed and has reached equilibrium (Seifert and Moldowan, 1986).

The values of the Ts/(Ts + Tm) and moretane/hopane (M/H) ratios obtained from the shale samples are highly variable among the five samples (Table 2). The equilibrium value for the Ts/(Ts + Tm) ratio is 0.52 to 0.55 (Seifert and Moldowan, 1986), although it is also governed by lithology and depositional environment (Peters et al., 2005). The M/H ratio decreases with thermal maturity from approximately 0.8 in immature bitumens to <0.15 in mature source rocks to a minimum of 0.05 (Mackenzie et al., 1980; Seifert and Moldowan, 1980); the ratio also depends on the facies and depositional environment (Peters et al., 2005). Thus, observed significant variations through the section in both the Ts/(Ts + Tm) and M/H ratios of the black shales studied suggest changes in organic matter input.

Based on pyrolysis and biomarker data -- 20S/(20S+20R) and ββ/(ββ +αα) sterane ratios -- and assuming there are no subtle differences in the maturity of the organic matter from the shales studied, the results indicate that the organic matter in the Namurian shales analysed is at the early mature to mid-mature stage.

Type of organic matter

Total organic carbon (TOC) measurements and Rock-Eval S2, HI and OI indices can be used to investigate the kerogen type, which in this case consists in general of a mixed assemblage of organic matter (Behar et al., 2001) (Table 1). Hydrogen indices range from 43 to 140 mg/kg, TOC varies from 0.37 to 2.45 (mean 1.57), and OI values range from 0 to 21 at Tmax of 436 to 454oC. These values suggest type III kerogen (Fig. 10, Table 1). A probable minor contribution of Type II kerogen which yields higher HI values of >300 can be inferred for at least one of the samples (1570.3 m) which plots in close proximity to the Type II boundary (Fig. 10). In general, Type III kerogens are composed of woody, bacterial and other sources of organic matter which have not undergone severe oxidative alteration. This terrestrial to mixed terrestrial - marine input of organic matter is broadly consistent with the basinal-prodelta depositional environment of the mudstones. Oxygen indices are low and invariant (0 to 21) which suggest that the organic matter has not undergone severe microbial decay or photochemical alteration. However, although measurement and interpretation of HI and OI values are useful, these values are influenced with increasing maturation and become less reliable as an interpretative tool as values approach the origin (Fig. 10).

Gas chromatograms of saturated hydrocarbons show a similar n-alkane distribution in the mudrock samples (Fig. 11), displaying a full suite of saturated hydrocarbons between C14-C39 n-alkanes and the isoprenoids pristane (Pr) and phytane (Ph). The n-alkane distributions exhibit a predominance of low to medium molecular weight compounds (n-C14 to n-C20) with the presence of significant waxy alkanes (+n-C27), suggesting a high contribution of marine organic matter with moderate terrigenous organic matter contribution (Eglinton et al., 1962).

Cross-plots of Pr/n-C17 versus Ph/n-C18 (Shanmugam, 1985) also suggest a mixed (terrestrial-marine) or terrestrial source of organic matter (Fig. 12).

370 Terpenoids are abundant with C19-C29 tricyclic terpanes and C30-C35 hopanes in all
371 samples (Fig. 13). The most probable biological precursors of the hopanoid biomarkers
372 are bacteriohopanetetrol and 3-desoxyhopanes (Ourisson et al., 1979; Rohmer et al.,
373 1992). Hopanes have also been reported as products of hopanoic acids (Bennett and
374 Abbott, 1999).
375
376 Of all steranes the C27 sterane is generally predominant (Fig. 13, Table 2). All of the
377 samples are characterized by similar C27/C29 (0.7 to 1.53) and C28/C29 (0.73 to 1.33)
378 sterane ratios. In general, C29 steranes are the major steroids derived from higher plants,
379 but significant quantities of C29 steranes can also be derived from a marine algal source
380 (e.g. Volkman, 2005). C27 steranes are commonly associated with zooplankton, and C28
381 steranes with chlorophyll-c containing phytoplankton (Huang and Meinschein, 1979).
382 However, Peters et al. (2005) and Volkman (2005) suggested caution in such
383 interpretations because many algae synthesize C29 sterols and there are many sources of
384 C27 and C28 sterols. Here, the distribution of C27-C28-C29 regular steranes shows a
385 slight dominance of C27 steranes (29-45 %), with slightly lower C29 (26-41 %), and
386 intermediate C28 (26-35 %) (Fig. 14, Table 2). The relative distributions of C27-C28-
387 C29 regular steranes are similar, but considerable variability within the proportions is
388 present in particular samples. Moreover, such variation is typical of Phanerozoic marine
389 source rocks (Grantham and Wakefield, 1988; Schwark and Empt, 2006). Therefore these
390 organic matter sources suggest that Namurian black shales contain marine algal and
391 terrigenous organic matter, with significant amounts of bacterial (microbially reworked)
392 organic matter.
393
394 Regular sterane/hopane ratios in Namurian shales show that the sterane abundance is
395 much lower than that of hopanes (0.05-0.27) which suggests a significant contribution of
396 prokaryotic organisms to the total biomass but is also consistent with terrestrial (soil)
397 inputs. A strong bacterial contribution is further confirmed by the high 2-methylhopane
398 index (2-MHP) which varies from 11.7 to 19.4 % (Table 2). The methylhopane index is
399 determined from the abundance of 2α-methyl-17α,21β(H)-hopane normalized to
400 17α,21β(H)-homohopane. The shale samples contain abundant 2α-methylhopanes,

401 ranging in carbon number from C29 to C32. Hopanoids methylated at the C-2 position
402 can be derived from cyanobacteria (Summons et al., 1999), but a recent study has shown
403 that their phylogenetic occurrence is potentially much broader (Welander et al., 2010).
404
405 Jarvie (2012) showed that marine-dominated shale gas resource systems (e.g. Barnett and
406 Fayetteville Shales, with moderate HI values of 30-40 mg hydrocarbon/g TOC) can be
407 excellent shale-gas targets. This is because at higher maturities the convertible carbon
408 fraction decreases when expulsion occurs. Therefore, determination of the original (post
409 burial) TOC and HI provides a more accurate means to asses organic matter quality and
410 generation potential. Comparison with immature shale rock equivalents showed original
411 HI of about >400 and original TOC of about 6%. However, in such settings, the organic
412 matter is mainly Type II (hydrogen rich) with high amounts of generative carbon.
413
414 In the present study, the black shales show considerable variability over a short depth
415 range but predominantly contain Type III kerogen and are not readily comparable to
416 organic matter deposited in deeper marine settings. Nevertheless, it is entirely reasonable
417 to assume that the low present-day TOC and HI values are an underestimate of original
418 values and that type III/II kerogen can yield significant amounts of oil and, to a lesser
419 extent, shale gas.
420
421 **REDOX NATURE OF THE DEPOSITIONAL ENVIRONMENT**
422
423 The Namurian shales in the Yorkshire area were deposited in a shallow-marine, pro-delta
424 environment as indicated by lithology and biomarker data. The Pr/Ph ratio varies from
425 0.3 to 3.04. This ratio has been used to infer depositional redox conditions (Maxwell et
426 al., 1972; Powell and McKirdy, 1973), but it is also influenced by factors such as thermal
427 maturity, variable biomolecule sources, lithology and diagenetic effects (e.g. Didyk et al.,
428 1978; ten Haven et al., 1987; Rowland, 1990; Kohnen et al., 1991; Hughes et al., 1995).
429 Therefore, the generally high Pr/Ph ratios in most samples indicate dysoxic to oxic
430 depositional conditions. Similarly, a cross-plot of Pr/n-C17 versus Ph/n-C18 ratios also
431 suggests deposition in dysoxic to oxic bottom waters (Fig. 12).

In these black shales, isorenieratane, which is derived from isorenieratene produced by brown-coloured green sulphur bacteria (Chlorobiaceae, Liaan-Jensen, 1978) and is therefore indicative of photic zone euxinia, is absent. Instead, low abundances of C18-C22 2,3,6-trimethyl aryl isoprenoids (Summons and Powell, 1987) were detected. These structures are diagenetic alteration products of isorenieratene, although they can also be derived from other carotenoids. Their trace concentrations precluded measurement of $\delta^{13}C$ values and confirmation of a green sulphur bacterial (Quandt et al., 1977; Sirevag et al., 1977; Koopmans et al., 1996; Jaraula et al., 2013) or algal source (Koopmans et al., 1996; Jaraula et al., 2013). However, as gammacerane and isorenieratane were not detected and the pristane/phytane ratio is in general >1, clear evidence for anoxia is lacking in all samples. A lack of profound water column anoxia is corroborated by the lack of high total organic carbon (TOC) content (0.3 – 2.4 wt%).

On the other hand, the presence of pyrite framboids, which are spherical aggregates of pyrite microcrystals and are similar to those in modern/ancient marine sediments, suggests deposition under oxygen-restricted conditions (Wilkin et al., 1996; 1997; Wignall and Newton, 1998). Hence, it is suggested that the Namurian mudrocks may have been deposited under conditions of periodic bottom water anoxia.

HYDROCARBON POTENTIAL

The hydrocarbon potential of the Malton-4 shales between 1568-1586 m depths can be assessed as a shale-gas resource or can be viewed from the standpoint of generating and retaining shale oil. The alternating shale-sandstone sequence suggests a hybrid system. As a classic unconventional play (i.e. self-sourced reservoir), gas could be sorbed by the mudstone-siltstone lithofacies; as a shale-oil system, oil could be generated and then migrate for a short distance to adjacent sandy mudrocks and bioturbated sands (Table 1; Fig. 5).

462 Setting aside these sedimentological considerations, prospective shale-gas plays, in
463 general have the following geochemical characteristics:
464
465 (i) good kerogen quality as determined from original hydrogen index values (HIo) of
466 250-800 mg/kg; (ii) high TOC >1.0 %; and (iii) thermal maturity of >1.4% VRo which is
467 equivalent to Tmax of about 500°C (e.g. Tmax °C = (VR % + 7.6) / (0.0180) (Andrews,
468 2013). Using Jarvie's (2007) HIo calculation and a not-unreasonable estimate of 50 %
469 Type II and 50 % Type III kerogen content, the Malton-4 black shales will have a HIo of
470 about 288 mg/g TOC. Combined with TOC values in the range of 0.37 to 2.46 %, These
471 values satisfy the basic organic geochemical characteristics of kerogen quality and
472 amount. However, the Tmax values (Table 2) suggest that the mudrocks analysed in this
473 study are too immature to be considered as a shale-gas resource. This does not
474 necessarily preclude limited gas generation, since small amounts of wet-gas are generated
475 in the early oil window.
476
477 The hydrocarbon potential of shale-oil systems can be assessed using the oil saturation
478 index (OSI: S1× 100 / TOC); potential resources are identified using empirical OSI
479 values >100 mg/g TOC. The premise here is that organic matter sorbs oil generated at
480 values <100 mg /g TOC and that the sorption threshold is exceeded at OSI >100 (the "oil
481 cross-over"). OSI values for the Malton-4 succession ranged from 4 to 17 mg/g TOC
482 (arithmetic mean 9 mg/g TOC), which falls well below the 100 mg cut-off and indicates
483 that the Upper Carboniferous mudrocks between (1569-1586 m depth) do not contain
484 enough oil to be considered a viable shale-oil resource.
485
486 **CONCLUSIONS**
487
488 The Upper Carboniferous succession studied in the Malton-4 well consists of four major
489 lithofacies: mudrock, sandy mudrock, bioturbated sandstone and massive sandstone. The
490 sandy mudrocks are shallower-water deposits and the presence of discrete muddy sand
491 beds with planar- and cross- lamination could indicate a storm influence (tempestites) or
492 distal fluvial hyperpycnal flows. The bioturbated sand facies indicates a distal to medial

493 mouth-bar setting whereas the more massive sands are interpreted to have been deposited
494 in a more proximal higher-energy location on a mouth bar.
495
496 Values of the total organic carbon content, and Rock-Eval S2, HI and OI indicate that
497 kerogen in general consists of type III material with a probable minor contribution of
498 Type II kerogen. This mixed terrestrial – marine (algal) and microbially reworked input
499 of organic matter is broadly consistent with the basinal-prodelta depositional environment
500 of the mudstones. Organic matter is at the early to mid-mature stage with respect to
501 hydrocarbon generation and was likely deposited in a mixed oxic-dysoxic-anoxic marine
502 environment.
503
504 The alternating shale-sandstone sequence suggests a hybrid system which could sorb gas
505 in the mudstone-siltstone Lithofacies, and could also generate shale oil which would
506 migrate a short distance to the sandy mudrocks and bioturbated sands. However, the
507 Rock-Eval parameters suggest that the mudrocks are not sufficiently mature to be
508 considered as a shale-gas resource and rule out a shale-oil potential. However this does
509 not preclude limited gas generation since small amounts of wet gas can be generated in
510 the early oil window.
511
512 ACKNOWLEDGEMENTS
513 To be added
514
515 **REFERENCES**
516
517 ABOUELRESH, M., SLATT, R.M., 2012. Lithofacies and sequence stratigraphy of the
518 Barnett Shale in east-central Fort Worth Basin, Texas. AAPG Bulletin, 96, 1-22.
519 ANDREWS, I.J., 2013. The Carboniferous Bowland Shale gas study: geology and
520 resource estimation. British Geological Survey for Department of Energy and Climate
521 Change, London, UK, 64 pp.

522 BEHAR, F., BEAUMONT, V., DE B. PENTEADO, H.L., 2001. Rock-Eval 6
523 technology: performances and developments. Oil and Gas Science and Technology, 56,
524 111-134.
525 BENNETT, B. AND ABBOTT, G.D., 1999. A natural pyrolysis experiment - hopanes
526 from hopanoid acids? Organic Geochemistry, 30, 1509-1516.
527 BOYER, C., CLARK, B., JOCHEN, V., LEWIS, R. AND MILLER, C.K., 2011. Shale
528 gas: A global resource. Oilfield Review, 23, 28-39.
529 BUNTING, P.J. AND BREYER, J.A., 2012. Lithology of the Barnett Shale
530 (Mississippian), southern Fort Worth Basin. In: J.A. Breyer, (Ed.), Shale reservoirs –
531 Giant resources for the 21st century. AAPG Memoir, 97, 322-343.
532 DEAN, M. T., BROWNE, M. A. E., WATERS, C. N. & POWELL, J. H. 2011. The
533 stratigraphical framework for the Carboniferous rocks of onshore northern Great Britain.
534 British Geological Survey Report R/10/07.
535 DIDYK, B.M., SIMONEIT, B.R.T., BRASSEL, S.C. AND EGLINTON, G., 1978.
536 Organic geochemical indicators of palaeonvironmental conditions of sedimentation.
537 Nature, 272, 216-222.
538 EGLINTON, G., GONZÁLEZ, A.G., HAMILTON, R. J. AND RAPHAEL, R. A., 1962.
539 Hydrocarbon constituents of the wax coatings of plant leaves: A taxonomic survey.
540 Phytochemistry, 1, 89–102.
541 ENGELHART, S.E., HORTON, B.P., HAWKES, A.D., WITTER, R.C., WANG, K.,
542 WANG, P-L. AND VANE, C.H. 2013. Testing the use of microfossils to reconstruct
543 great earthquakes at Cascadia. Geology, 41, 1067-1070.
544 FRASER, A.J. AND GAWTHORPE, R.L., 1990. Tectono-stratigraphic development and
545 hydrocarbon habitat of the Carboniferous in northern England. In: R.F.P. Hardman and J.
546 Brooks (Eds.), Tectonic Events for Britain's Oil and Gas Reserves, Geological Society,
547 London, Special Publication, 55, 49-86.
548 FRASER, A.J. AND GAWTHORPE, R.L., 2003. An Atlas of Carboniferous Basin
549 Evolution in Northern England. Geological Society Memoir, 28, 88pp.
550 GAWTHORPE, R.L., GUTTERIDGE, P. AND LEEDER, M.R. 1989. Late Devonian
551 and Dinantian basin evolution in northern England and North Wales. In: Arthurton, R.S.,
552 GUTTERIDGE, P. AND NOLAN, S. C. (Eds.), The Role of Tectonics in Devonian and
553 Carboniferous Sedimentation in the British Isles. Yorkshire Geological Society
554 Occasional Publication, 6, 1–23.
555 GEORGE, T.N., JOHNSON, G.A.L, MITCHELL, M., PRENTICE, J.E.,
556 RAMSBOTTOM, W.H.C., SEVASTOPULO, G.D. AND WILSON, R. 1976. A

557 Correlation of the Dinantian rocks of the British Isles. Special Report, Geological Society
558 of London, 7, 1–87.
559 GRADSTEIN, F.M., OGG, J.G., SCHMITZ, M. AND OGG, G., 2012. The Geologic
560 Time Scale 2012. Elsevier, Amsterdam.
561 GRANTHAM, P.J. AND WAKEFIELD, L.L., 1988. Variations in the sterane carbon
562 number distributions of marine source rock derived crude oils through geological time.
563 Organic Geochemistry, 12, 61-73.
564 HUGHES, W.B., ALBERT, T., HOLBA, G. AND DZOU, L., 1995. The ratios of
565 dibenzothiphene to phenanthrene and pristane to phytane as indicators of depositional
566 environment and lithology of petroleum source rocks. Geochimica et Cosmochimica
567 Acta, 59, 3581-3598.
568 JARAULA, C.M.B., GRICE, K., TWITCHETT, R.J., BÖTTCHER, M.E.,
569 LEMETAYER, P., DASTIDAR, A.G. AND OPAZO, L.F., 2013. Elevated pCO2 leading
570 to Late Triassic extinction, persistent photic zone euxinia, and rising sea levels. Geology,
571 41, 955-958.
572 JARVIE, D.M., BURGESS, J.D., MORELOS, A., MARIOTTI, P.A. AND LINDSEY,
573 R., 2001. Permian Basin petroleum systems investigations: inferences from oil
574 geochemistry and source rocks. AAPG Bulletin, 85, 1693-1694.
575 JARVIE, D.M., 2012. Shale resource systems for oil and gas: Part 1 – Shale-gas resource
576 systems. In: J.A. Breyer, (Ed.), Shale reservoirs – Giant resources for the 21st century.
577 AAPG Memoir, 97, 69-87.
578 JOHNSON, G.A.L., 1984. Subsidence and sedimentation in the Northumberland
579 Trough. Proceedings of the Yorkshire Geological Society, 45, 71–83.
580 JOHNSON, G.A.L., SOMERVILLE, I.D., TUCKER, M.E. AND COZAR, P., 2011.
581 Carboniferous stratigraphy and context of the Seal Sands No. 1 Borehole, Teesmouth, NE
582 England: the deepest onshore borehole in Great Britain. Proceedings of the Yorkshire
583 Geological Society, 58, 173-196.
584 KODRANS-NSIAH, M., MÄRZ, C., HARDING, I.C., KASTEN, S. AND
585 ZONNEVELD, K.A.F., 2009. Are the Kimmeridge Clay deposits affected by 'burn-
586 down' events? Palynological and geochemical studies on a 1 metre long section from the
587 Upper Kimmeridge Clay Formation (Dorset, UK). Sedimentary Geology, 222, 301-313.

KOHNEN, M.E.L., SINNINGHE DAMSTÉ, J.S. AND DE LEEUW, J.W., 1991. Biases from natural sulphurization in palaeoenvironmental reconstruction based on hydrocarbon biomarker distributions. Nature, 349, 775-778.

KOOPMANS, M.P., SCHOUTEN, S., KOHNEN, M.E.L. AND SINNINGHE DAMSTÉ, J., 1996. Restricted utility of aryl isoprenoids as indicators for photic zone anoxia. Geochimica et Cosmochimica Acta, 60, 4873-4876.

LIAAN-JENSEN, S., 1978. Chemistry of carotenoid pigments. In: R.K. Clayton and W.R. Sistrom, (Eds.), Photosynthetic Bacteria. Plenum Press, New York, pp. 233-247.

MACKENZIE, A.S., PATIENCE, R.L. AND MAXWELL, J.R., 1980. Molecular parameters of maturation in the Toarcian shales, Paris Basin, France: I. Changes in the configurations of acyclic isoprenoid alkanes and triterpanes. Geochimica et Cosmochimica Acta, 44, 1709-1721.

MAXWELL, R.E., COX, R.G., ACKMAN, R.G. AND HOOPER, S.N., 1972. The diagenesis and maturation of phytol. The stereochemistry of 2,6,10,14-tetramethylpentadecane from an ancient sediment. In: H.R. von Gartner and H. Wehner, (Eds.), Advances in Organic Geochemistry, pp. 177-291.

OURISSON, G., ALBRECHT, P. AND ROHMER, M., 1979. The hopanoids: palaeochemistry and biochemistry of a group of natural products. Pure and Applied Chemistry, 51, 709-729.

PETERS, K.E. AND CASSA, M.R., 1994. Applied source rock geochemistry. In: L.B. Magoon and W.G. Dow, (Eds.), Petroleum System – From Source to Trap. AAPG Memoir, 60, 93-117.

PETERS, K.E., WALTERS, C.C. AND MOLDOWAN, J.M., 2005. The Biomarker Guide: II. Biomarkers and Isotopes in Petroleum Exploration and Earth History, 2nd edition. Cambridge University Press, Cambridge, pp. 1-706.

PLINT, A.G., 2014. Mud dispersal across a Cretaceous prodelta: Storm-generated wave-enhanced sediment gravity flows inferred from mudstone microtexture and microfacies. Sedimentology, 61, 609-647.

POWELL, T.G. AND MCKIRDY, D.M., 1973. Relationship between ratio of pristane to phytane, crude oil composition and geological environment in Australia. Nature, 243, 37-39.

619 QUANDT, I., GOTTSHALK, G., ZIEGLER, H. AND STICHLER, W., 1977. Isotope
620 discrimination by photosynthetic bacteria. FEMS Microbiology Letters, 1, 125-128.
621 ROBINSON, S.G., 2001. Early diagenesis in an organic-rich turbidite and pelagic clay
622 sequence from the Cape Verde Abyssal Plain, NE Atlantic: magnetic and geochemical
623 signals. Sedimentary Geology, 143, 91-123.
624 ROHMER, M., BISSERET, P. AND NEUNLIST, S., 1992. The hopanoids, prokaryotic
625 triterpenoids and precursors of ubiquitous molecular fossils. In: J.M. Moldowan, P.
626 Albrecht and R.P. Philp, (Eds.), Biological Markers in Sediments and Petroleum. Prentice
627 Hall, Englewood Cliffs, NJ, pp. 1-17.
628 ROWLAND, S.J., 1990. Production of acyclic isoprenoid hydrocarbons by laboratory
629 maturation of methanogenic bacteria. Organic Geochemistry, 15, 9-16.
630 SCHWARK, L. AND EMPT, P., 2006. Sterane biomarkers as indicators of Palaeozoic
631 algal evolution and extinction events. Palaeogeography, Palaeoclimatology,
632 Palaeoecology, 240, 225-236.
633 SEIFERT, W.K. AND MOLDOWAN, J.M., 1986. Use of biological markers in
634 petroleum exploration. In: R.B. Johns, (Ed.), Methods in Geochemistry and Geophysics,
635 24, 261-290.
636 SHANMUGAM, G., 1985. Significance of coniferous rain forests and related organic
637 matter in generating commercial quantities of oil, Gippsland Basin, Australia. AAPG
638 Bulletin, 69, 1241-1254.
639 SIREVAG, R., BUCHANAN, B.B., BERRY, J.A. AND THROUGHTON, J.H., 1977.
640 Mechanisms of CO2 fixation in bacterial photosynthesis studied by the carbon isotope
641 technique. Archives of Microbiology, 112, 35-38.
642 SMITH, N., TURNER, P. AND WILLIAMS, G., 2011. UK data and analysis for shale
643 gas prospectivity. In: Vining, B.A., Pickering, S.C. (eds), Petroleum Geology: From
644 Mature Basins to New Frontiers – Proceedings of the 7th Petroleum Geology Conference.
645 Geological Society London, Petroleum Geology Conference Series, 7, 1087-1098.
646 SUMMONS, R.E. AND POWELL, T.G., 1987. Identification of aryl isoprenoids in
647 source rocks and crude oils: biological markers for green photosynthetic bacteria.
648 Geochimica et Cosmochimica Acta, 51, 557-566.

649 SUMMONS, R.E., JAHNKE, L.L., HOPE, J.M. AND LOGAN, G.A., 1999. 2-
650 Methylhopanoids as biomarkers for cyanobacterial oxygenic photosynthesis. Nature, 400,
651 554-557.
652 TEN HAVEN, H.L., DE LEEUW, J.W., RULLKÖTTER, J. AND SINNINGHE-
653 DAMSTÉ, J., 1987. Restricted utility of the pristane/phytane ratio as a
654 palaeoenvironmental indicator. Nature, 330, 641-643.
655 THOMSON, J., HIGGIS, N.C., WILSON, T.R.S., CROUDACE, I.W., DELANGE, G.J.
656 AND VANSANTVOORT, P.J.M., 1995. Redistribution and geochemical behaviour of
657 redox-sensitive elements around S1, the most recent eastern Mediterranean sapropel.
658 Geochimica et Cosmochimica Acta, 59, 3487-3501.
659 TUCKER, M.E., GALLAGHER, J. AND LENG, M., 2009. Are beds millennial-scale
660 cycles? An example from the Carboniferous of NE England. Sedimentary Geology, 214,
661 19-34.
662 VOLKMAN, J.K., 2005. Sterols and other triterpenoids: source specificity and evolution
663 of biosynthetic pathways. Organic Geochemistry, 36, 139-159.
664 WATERS, C.N. BROWNE, M.A.E., DEAN, M.T. AND POWELL, J.H. 2007.
665 Lithostratigraphical framework for Carboniferous successions of Great Britain (onshore).
666 British Geological Survey Report.
667 WELANDER, P.V., COLEMAN, M.L., SESSIONS, A.L., SUMMONS, R.E. AND
668 NEWMAN, D.K., 2010. Identification of a methylase required for 2-methylhopanoid
669 production and implications for the interpretation of sedimentary hopanes. PNAS, 107,
670 8537-8542.
671 WIGNALL, P.B. AND NEWTON, R., 1998. Pyrite framboid diameter as a measure of
672 oxygen deficiency in ancient mudrocks. American Journal of Science, 298, 537-552.
673 WILKIN, R.T., BARNES, H.L. AND BRANTLEY, S.L., 1996. The size distribution of
674 framboidal pyrite in modern sediments: an indicator of redox conditions. Geochimica et
675 Cosmochimica Acta, 60, 3897-3912.
676 WILKIN, R.T., ARTHUR, M.A. AND DEAN, W.E., 1997. History of water-column
677 anoxia in the Black Sea indicated by pyrite framboid size distributions. Earth and
678 Planetary Science Letters, 148, 517-525.
679
680 Figure captions:

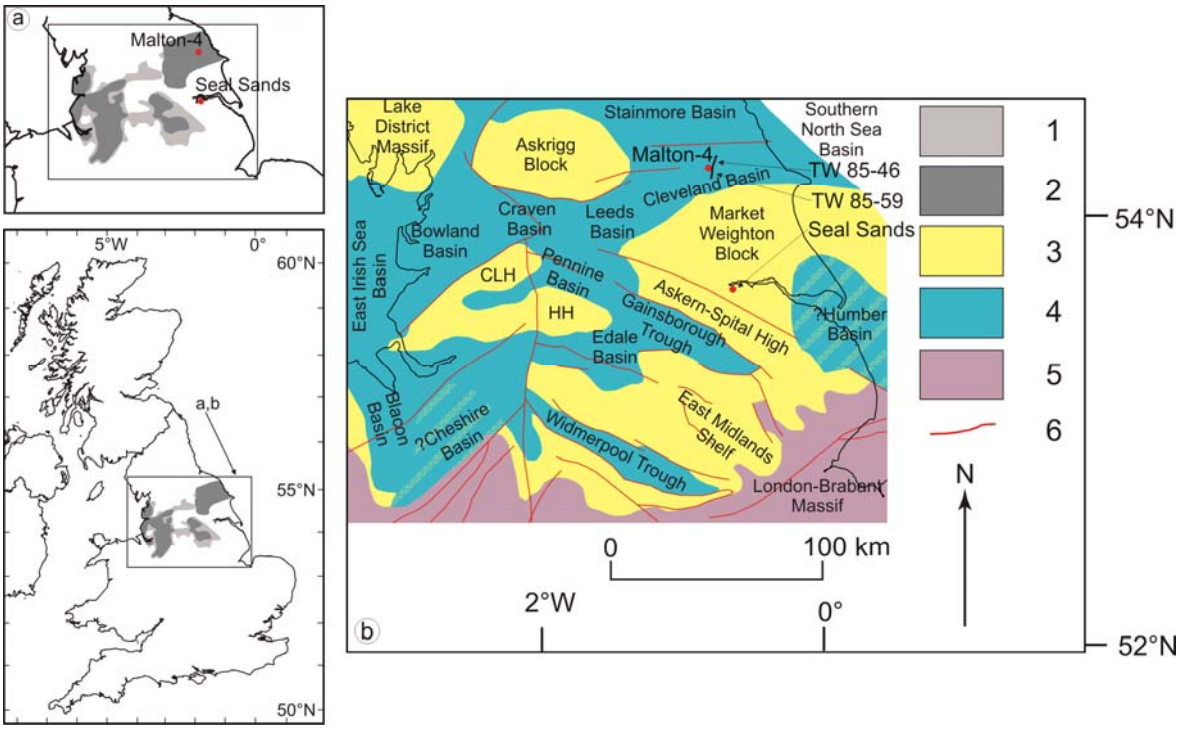

Fig. 1A. Location of Malton-4 well [not located in this figure] and prospective areas for shale gas in the Bowland-Hodder unit in the northern England (after Andrews, 2013). Also shown are the locations of the seismic lines presented in Fig. 1b. Key: 1. prospective area for gas in lower (Visean) Bowland-Hodder unit; 2. prospective area for gas in upper (Namurian) Bowland-Hodder unit

B. Palaeogeography of northern England during the mid-Carboniferous showing the location of blocks and basins (modified from Fraser and Gawthorpe, 2003).

Key: 3. platform; 4. basin; 5. basement high; 6. fault; CLH - Central Lancashire High; HH - Holme High.

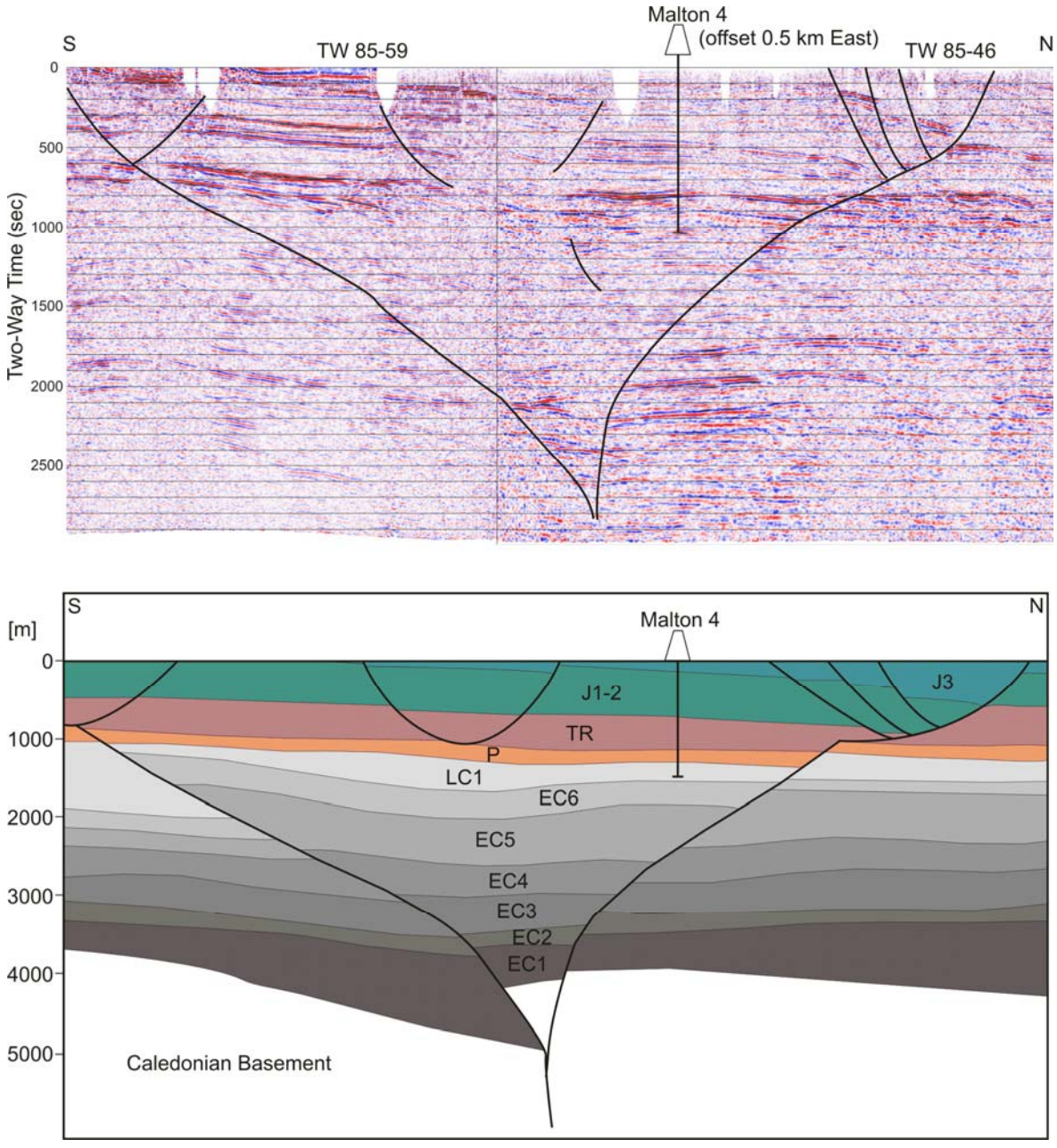

Fig. 2. Geological cross-section interpreted from seismic lines TW 85-46 and TW 85-59 across the Cleveland Basin (simplified from Fraser and Gawthorpe, 2003). J1-2: Early-

Middle Jurassic; J3: Late Jurassic; TR: Triassic; P: Permian; LC1: Namurian seismic stratigraphic cycles; EC1 to EC6: Mississippian seismic stratigraphic cycles. See Fig. 3 for the lithostratigraphy.

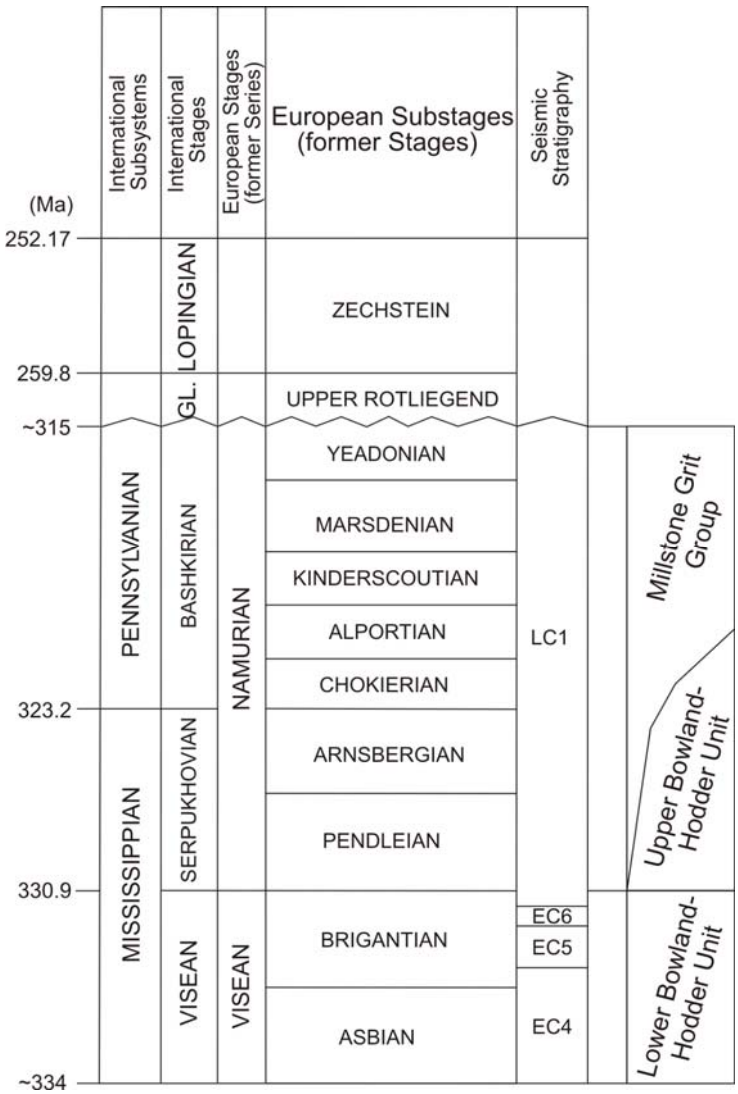

Fig. 3. Chronostratigraphic framework for the Carboniferous and Permian in the study area. Seismic sequences from Fraser et al. (1990). GL – Guadalupian. Numerical ages for all systems are after Gradstein et al. (2012).

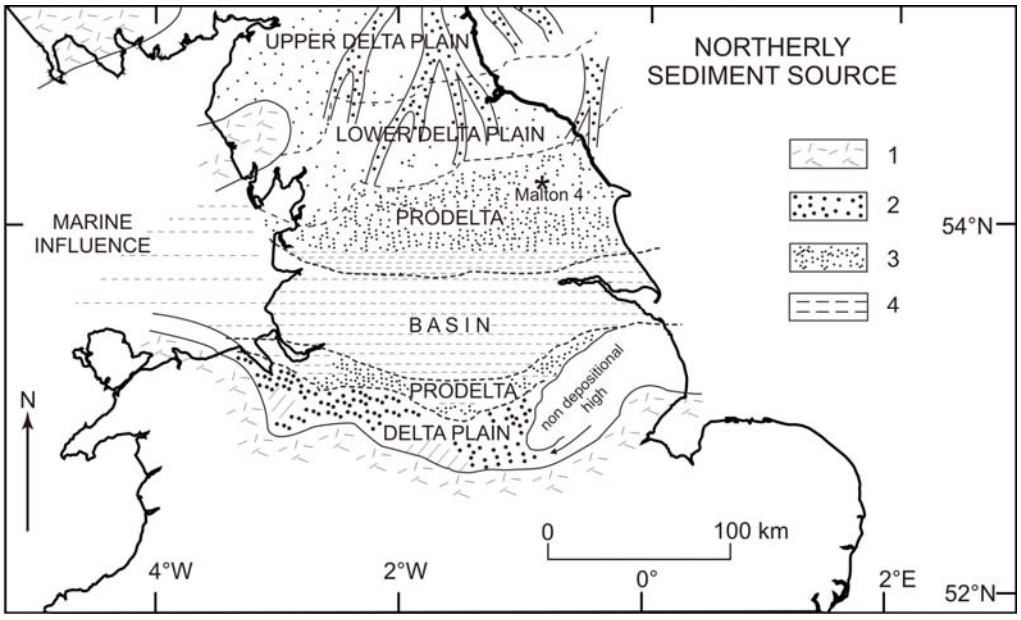

Fig. 4. Palaeofacies map for the post-rift LC1a/b sequence (Arnsbergian-Kinderscoutian) in northern England (modified after Fraser and Gawthorpe, 1990). 1, Lower Palaeozoic/Precambrian basement; 2, coarse, mostly fluvial clastics; 3, finer sandstones and mudrocks, local coals; 4, mudrocks, locally organic-rich shales.

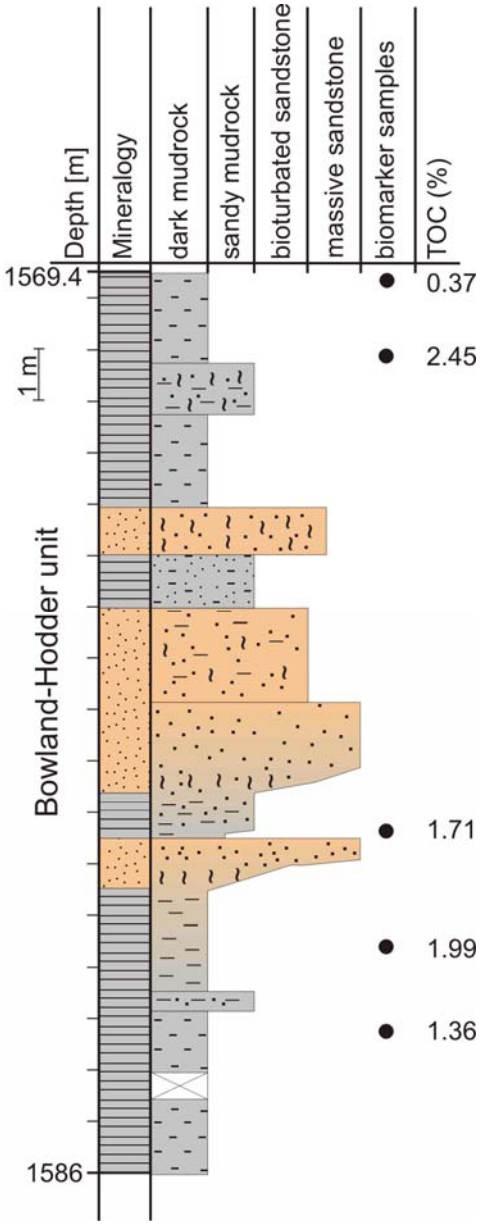

Fig. 5. Sedimentary log of Upper Carboniferous mudrocks and sandstones from the Malton-4 well.

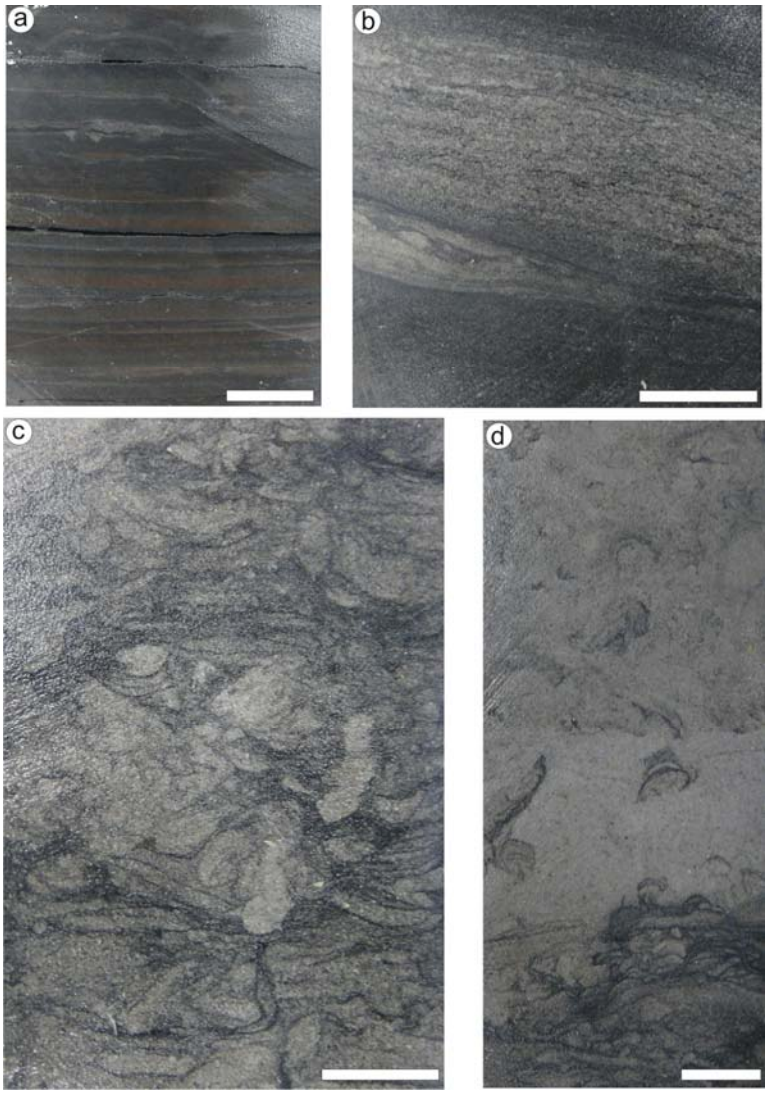

Fig. 6. Sedimentary features in samples from the Malton-4 well. (a) Black shale with mm-lamination and no bioturbation; (b) Mudrock with 5-cm thick tempestite / hyperpycnite siltstone-fine sandstone from pro-delta facies; (c) Bioturbated, muddy fine sandstone with Planolites, Chondrites and Thalassinoides burrows; (d) Bioturbated muddy to clean sand with Chondrites, Pelecypodichnus and Planolites burrows. Scale bars 2 cm.

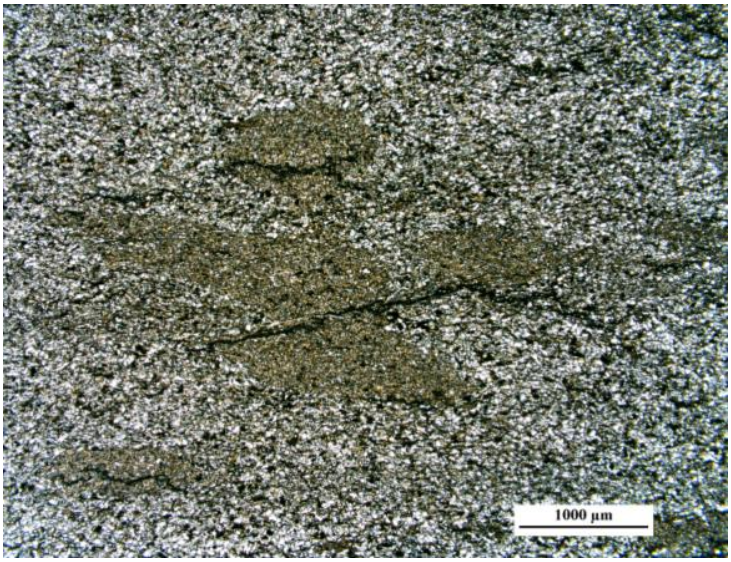

752

753 Fig. 7. Silty mudrock with silt-poor areas which are probably burrow fills. Discontinuous

754 irregular stylolitic seams show concentrations of organic matter.

755

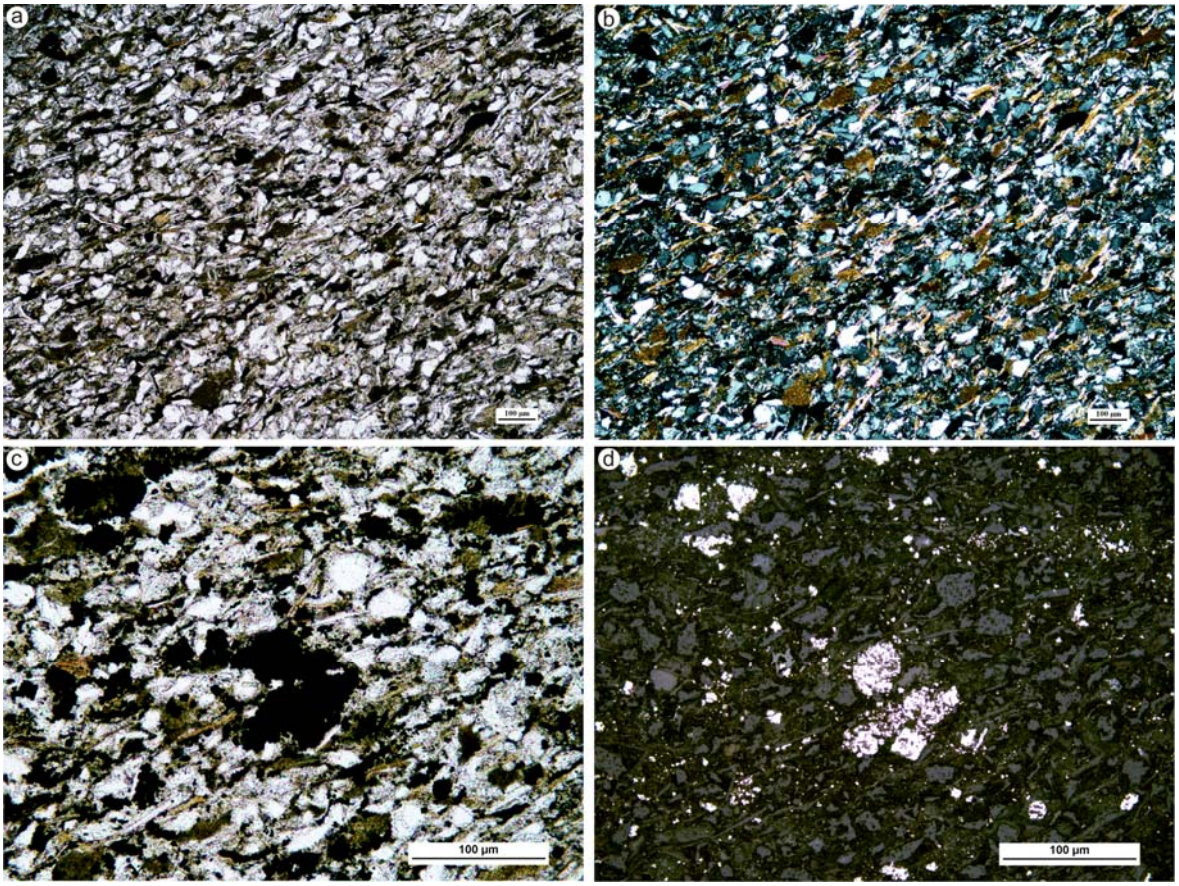

756

757 Fig. 8. Mudrock in plane-polarized light (a) and crossed-polarized light (b) showing
758 quartz silt grains (~30%), mica (~5%, mostly muscovite), opaque/black pyrite and
759 organic matter (~5%), and clay matrix, altered feldspar and other grains (60%). Mudrock
760 in plane-polarized light (c) and reflected light (d) showing that some of the opaque grains
761 are pyrite (white in D); other black areas are organic matter. White arrows point
762 microporosity. In the photomicrographs, lamination is oriented NE-SW.
763

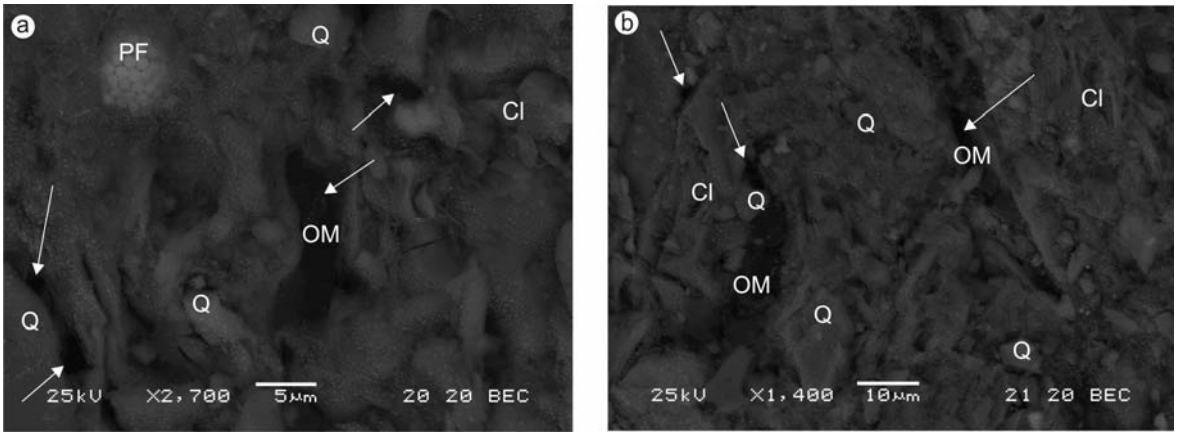

764
765 Fig. 9. Back-scattered scanning electron microscopic images of Upper Carboniferous
766 mudrock; lamination oriented north-south. (a) higher magnification showing organic
767 material in centre, pyrite framboid (upper left), clay, fine-silt quartz grains and nano-
768 pores; (b) shows two fragments of organic matter (dark elongate areas), fine, silt-sized
769 quartz grains, and clay flakes. Nano-pores are present between some grains; OM -
770 organic material, Q - quartz, Cl - clay, PF - pyrite framboid.
771
772
773
774

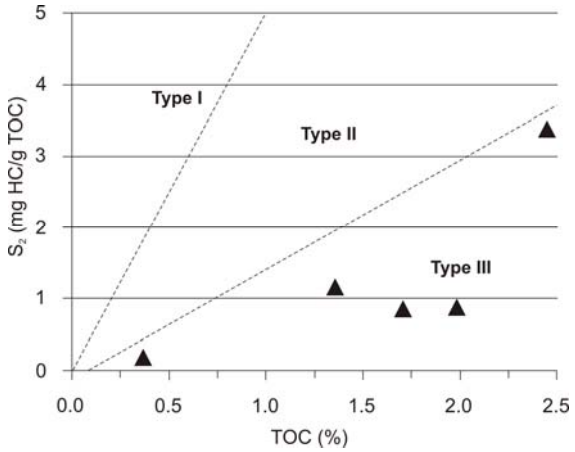

775

776 Fig. 10. Kerogen type in Malton-4 succession defined by present-day S2-TOC cross-plot.

777

778

779

780

781

782

783

784

785

786

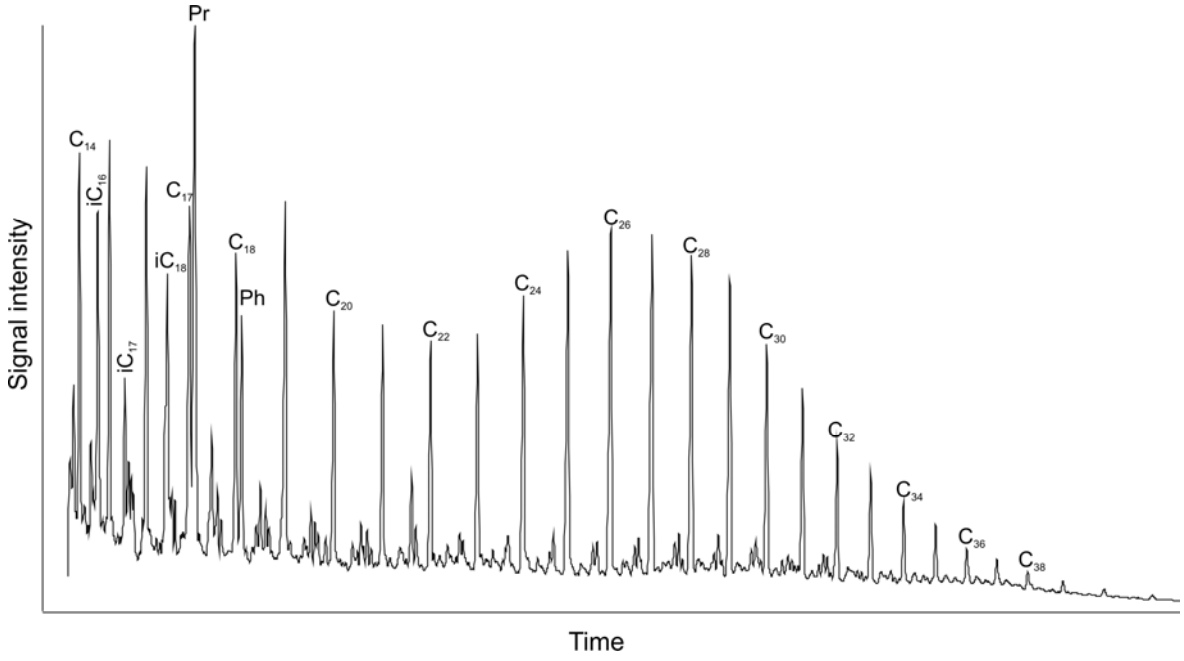

Fig. 11. Gas chromatogram of saturated hydrocarbons of the studied Namurian shale extracts. iC16-18 – acyclic isoprenoids; Pr – pristane; Ph – phytane.

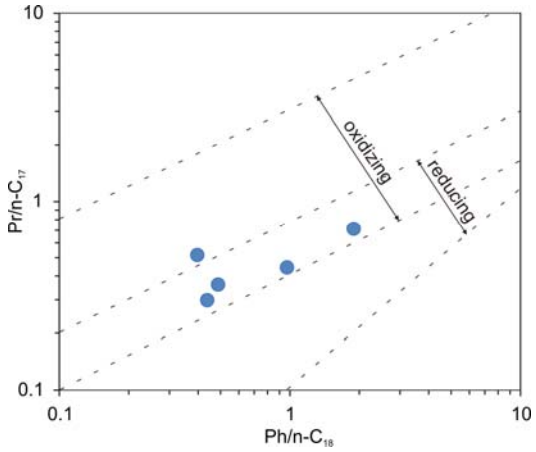

Fig. 12. Pr/n-C17 vs. Ph/n-C18 plot for all samples indicating deposition under oxidizing to oxygen-depleted conditions.

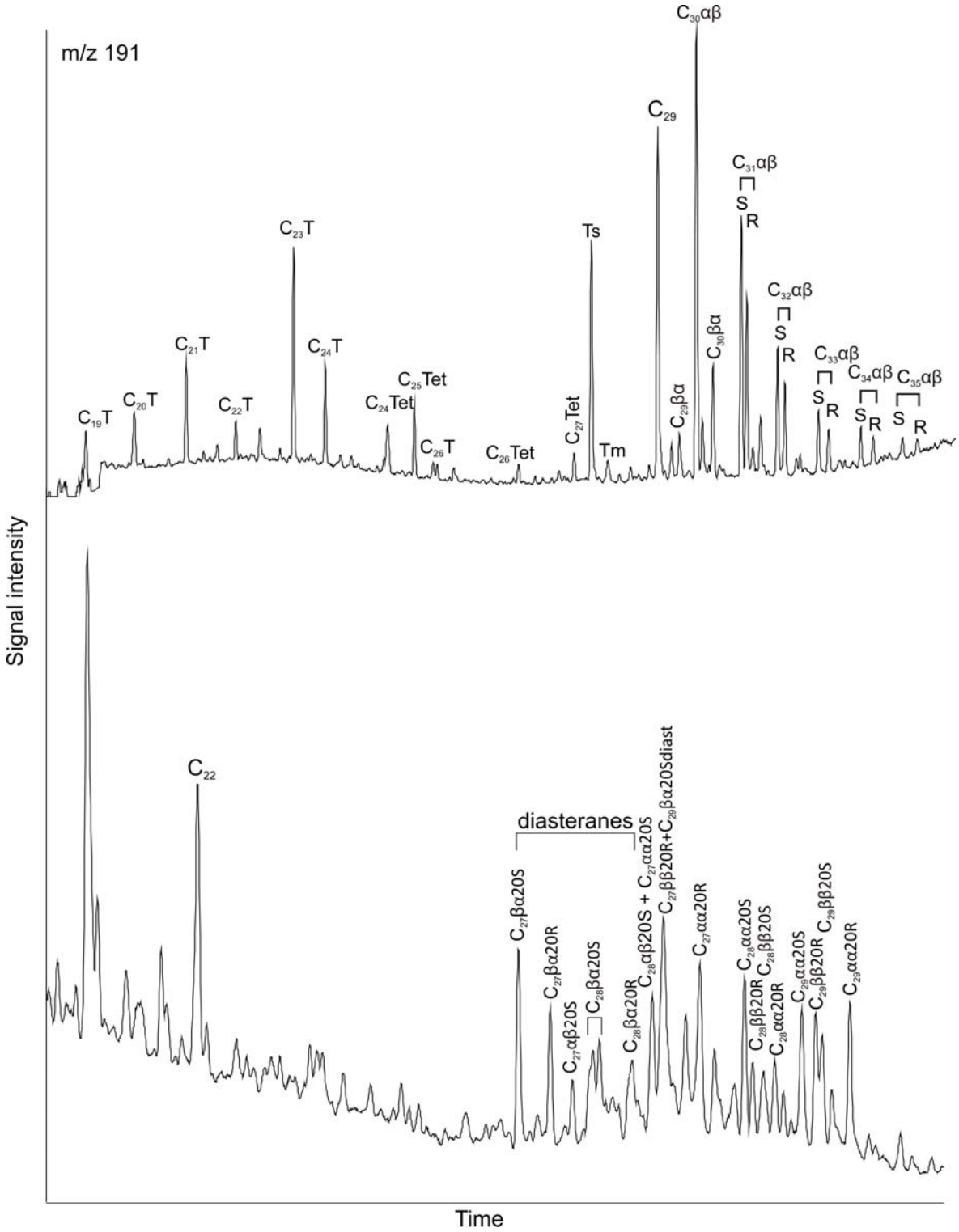

795

796 Fig. 13. The m/z 191 and m/z 217 mass chromatograms of saturated hydrocarbon
797 fractions of the analysed Namurian shale extracts. C19-26T – tricyclic terpenoids; C25-
798 27Tet – tetracyclic terpenoids; Ts - C27 18α-trisnorhopane; Tm - C27 17α-trisnorhopane.

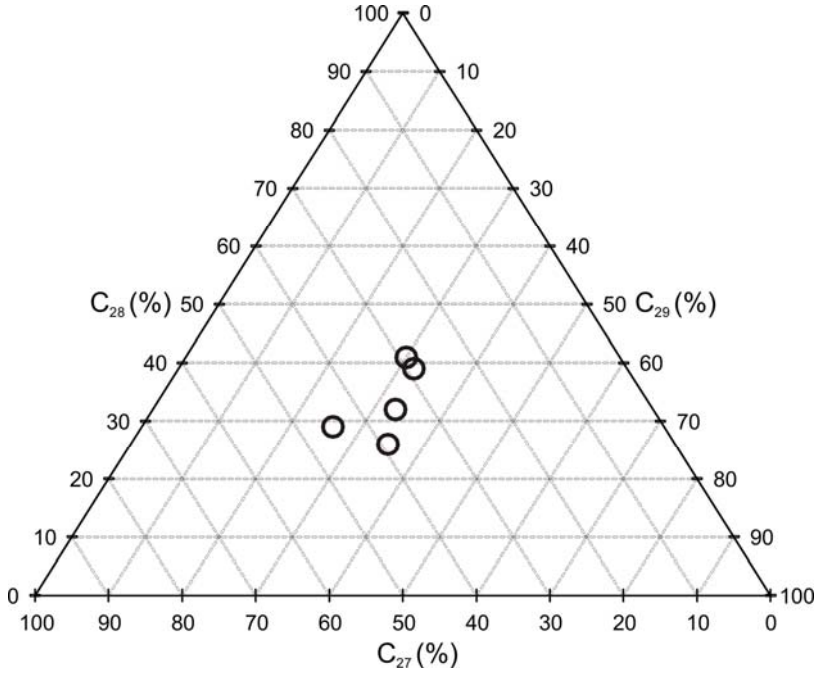

Fig. 14. A ternary plot of C27 vs. C28 vs. C29 regular steranes (as normalised percentages) for the Carboniferous mudrocks.

Depth (m)	TOC[a] (%)	S_1[b] (mg HC/ g rock)	S_2[b] (mg HC/ g rock)	T_{max}[d] (^oC)	HI[e] (mg HC/ g rock)	OI[f] (mg g/ g rock)	PI[g] ($S_1/(S_1+S_2)$)
1569.5	0.37	0.02	0.20	443	53	30	0.05
1570.3	2.45	0.43	3.38	436	138	4	0.11
1579.5	1.71	0.13	0.87	451	51	16	0.13
1581.3	1.99	0.15	0.89	454	45	12	0.15
1583.1	1.36	0.14	1.17	440	87	21	0.11

Table 1. Results of total organic carbon analyses (TOC) and Rock-Eval pyrolysis for the shale samples from Malton 4.

aTOC, total organic carbon

bS1, volatile hydrocarbon (HC) content, mg HC/g rock

cS2, remaining HC generative potential, mg HC/g rock

dTmax, temperature at maximum of S2 peak

813 eHI, hydrogen index

814 fOI, oxygen index

815 gPI, production index.

816

Depth (m)	Pr/Ph[a]	Pr/n-C_{17}	Ph/n-C_{18}	Ts/Tm[b]	M/H[c]	HHI[d]	C_{29} ααα S/(S+R)[e]	C_{29} ββ/ (ββ +αα)[f]	C_{27}/C_{29}[e]	C_{28}/C_{29}[f]	$C_{27, 28, 29,}$ steranes	Sterane/ hopane	2-MHP[g]
1569.5	0.31	0.37	0.51	0.55	0.19	0.14	0.47	0.42	1.11	1.03	32, 33, 35	0.27	11.72
1570.3	3.04	1.89	0.71	0.28	0.19	0.04	0.56	0.48	1.53	0.88	29, 26, 45	0.19	11.81
1579.5	1.05	0.48	0.35	nd	0.24	0.06	0.47	0.46	0.76	0.83	39, 32, 29	0.09	13.02
1581.3	0.86	0.43	0.29	0.11	0.27	0.04	0.42	0.40	0.70	0.73	41, 30, 29	0.05	12.26
1583.1	2.07	0.97	0.44	0.66	0.16	0.06	0.53	0.55	1.50	1.33	26, 35, 39	0.11	19.46

817

818

819 Table 2. Overview of geochemical parameters measured and discussed in this study. nd –

820 not determined.

821 a Pr/Ph: pristane / phytane ratio

822 b Ts/Tm: C27 17α-trisnorhopane (Tm) / C27 18α-trisnorhopane ratio expressed as

823 Ts/(Ts+Tm)

824 c M/H (moretane/hopane ratio): 17β(H),21α(H) – moretane/17α(H),21β(H) – hopane

825 d HHI (homohopane index): C35αβ(22S+22R) / (ΣC31-C35 αβ 22S+22R)

826 e,f C27/C29 and C28/C29 are sterane ratios respectively

827 g 2-MHP: C32 2α-methylhopanes (22S + 22R) / C31 (22R) homohopane

828